

Cathepsin B Overexpression Due to Acid Sphingomyelinase Ablation Promotes Liver Fibrosis in Niemann-Pick Disease*

Received for publication, June 15, 2011, and in revised form, November 1, 2011. Published, JBC Papers in Press, November 18, 2011, DOI 10.1074/jbc.M111.272393

Anna Moles^{†1}, Núria Tarrats^{†1}, José C. Fernández-Checa^{‡§2,3}, and Montserrat Mari^{†2,4}

From the [†]Institut d'Investigacions Biomèdiques August Pi i Sunyer, Liver Unit-Hospital Clínic, Centro de Investigación Biomédica en Red en el Área Temática de Entermedades Hepáticas y Digestivas, and Department of Cell Death and Proliferation, Instituto de Investigaciones Biomédicas de Barcelona, Consejo Superior de Investigaciones Científicas, 08036 Barcelona, Spain and the [§]Research Center for Alcoholic Liver and Pancreatic Diseases, Keck School of Medicine, University of Southern California, Los Angeles, California 90089

Background: The mechanism of liver fibrosis in Niemann-Pick disease (NPD) is unknown.

Results: The loss of ASMase stimulates cathepsin B (CtsB) activation promoting liver fibrosis.

Conclusion: CtsB contributes to the hepatic phenotype of NPD.

Significance: CtsB may be a novel therapeutic target to treat liver disease in NPD.

Niemann-Pick disease (NPD) is a lysosomal storage disease caused by the loss of acid sphingomyelinase (ASMase) that features neurodegeneration and liver disease. Because ASMase-knock-out mice models NPD and our previous findings revealed that ASMase activates cathepsins B/D (CtsB/D), our aim was to investigate the expression and processing of CtsB/D in hepatic stellate cells (HSCs) from ASMase-null mice and their role in liver fibrosis. Surprisingly, HSCs from ASMase-knock-out mice exhibit increased basal level and activity of CtsB as well as its *in vitro* processing in culture, paralleling the enhanced expression of fibrogenic markers α -smooth muscle actin (α -SMA), TGF- β , and pro-collagen- α 1(I) (Col1A1). Moreover, pharmacological inhibition of CtsB blunted the expression of α -SMA and Col1A1 and proliferation of HSCs from ASMase-knock-out mice. Consistent with the enhanced activation of CtsB in HSCs from ASMase-null mice, the *in vivo* liver fibrosis induced by chronic treatment with CCl₄ increased in ASMase-null compared with wild-type mice, an effect that was reduced upon CtsB inhibition. In addition to liver, the enhanced proteolytic processing of CtsB was also observed in brain and lung of ASMase-knock-out mice, suggesting that the overexpression of CtsB may underlie the phenotype of NPD. Thus, these findings reveal a functional relationship between ASMase and CtsB and that the ablation of ASMase leads to the enhanced processing and activation of CtsB. Therefore, targeting CtsB may be of relevance in the treatment of liver fibrosis in patients with NPD.

Acid sphingomyelinase (ASMase⁵; EC 3.2.1.14) is a member of an enzyme family that catalyzes the breakdown of sphingomyelin into ceramide. ASMase works optimally at acidic pH and is located mainly in the endo/lysosomal compartments (1). Besides its important participation as key structural component of biological membranes, ceramide is recognized as a critical second messenger that regulates many cell functions (2, 3). In particular, ceramide generation by ASMase is rapid and transient and plays a proapoptotic role in response to many different stimuli (2, 3). ASMase derives from a pro-inactive form whose proteolytic processing within the C terminus leads to the maturation of an endosomal/lysosomal Zn²⁺-independent form and a Zn²⁺-dependent secretory isoenzyme (4).

Niemann-Pick disease (NPD) is a rare lysosomal storage disorder caused by recessive mutations on the *SPMD1* gene encoding ASMase (5, 6). NPD type A and B, the most common subtypes of this disease, share features such as the accumulation of sphingomyelin, cholesterol, glycosphingolipids, and bis-(monoacylglycerol) phosphate in the visceral organs such as liver, spleen, and lung. The subsequent formation of foam cells is the main cause of hepatosplenomegaly, pulmonary insufficiency, and cardiovascular disease (6). NPD type A patients typically exhibit almost a total loss of ASMase activity and suffer neurological degeneration that reduces their lifespan to about 3 years of age. NPD type B patients, however, frequently survive into adulthood and exhibit a milder phenotype with little or no neurodegeneration depending on the remaining percentage of ASMase activity (7). Despite the generation of the ASMase-knock-out mice as an animal model of NPD type A exhibiting neurological degeneration, hepatosplenomegaly, and lung dysfunction (8, 9), little progress has been made in NPD treatment.

Cathepsins are a family of lysosomal proteases whose participation in different pathologies such as liver fibrosis (10), ath-

* The work was supported, in whole or in part, by Grant P50-AA-11999 from the Research Center for Liver and Pancreatic Diseases, National Institute on Alcohol Abuse and Alcoholism. This work was carried out in part at the Esther Koplowitz Center in Barcelona, and it was also supported by Grants PI10/02114 (Instituto de Salud Carlos III), 2009-11417 (Plan Nacional de I+D), Spain; and the and Fundació La Marató de TV3.

¹ Both authors contributed equally to this work.

² Both authors share senior authorship.

³ To whom correspondence may be addressed: Liver Unit, Hospital Clínic, C/Villarroel 170, 08036 Barcelona, Spain. Tel.: 34-93-227-5709; E-mail: checa229@yahoo.com.

⁴ To whom correspondence may be addressed: Liver Unit, Hospital Clínic, C/Villarroel 170, 08036 Barcelona, Spain. Tel.: 34-93-227-5709; E-mail: monmari@clinic.ub.es.

⁵ The abbreviations used are: ASMase, acid sphingomyelinase; α -SMA, α -smooth muscle actin; CCl₄, carbon tetrachloride; Col1A1, pro-collagen- α 1(I); CtsB, cathepsin B; CtsD, cathepsin D; EWAT, epididymal white adipose tissue; HSC, hepatic stellate cell; NPD, Niemann-Pick disease.

erosclerosis (11), Alzheimer disease (12), and cancer (13, 14) has been reported in the past years. In particular, cathepsin B (CtsB) and cathepsin D (CtsD) have been implicated in signaling pathways of apoptosis (15, 16) and liver fibrosis (17). Moreover, recent studies have revealed that ASMase controls the proteolytic processing of CtsB/D, and hence ASMase down-regulation impairs CtsB/D processing resulting in decreased hepatic stellate cell (HSC) activation *in vitro* and lower *in vivo* fibrogenesis (17). However, because many cathepsins are proteolytically processed by other members of the family and due to the hierarchical relationship between ASMase and CtsB/D (17), we postulated that the complete loss of ASMase may lead to an adaptive overexpression of CtsB/D. To test this hypothesis we addressed the regulation of CtsB/D in ASMase-knock-out mice and examined the activation of HSCs *in vitro* and liver fibrosis *in vivo* as a potential contributory mechanism for enhanced liver disease observed in many NPD patients (18–21). Moreover, because the NPD phenotype is not restricted to liver, we addressed the regulation of CtsB/D in other commonly affected organs of ASMase-knock-out mice. Our findings revealed an increased proteolytic processing of CtsB/D in HSC from ASMase-null mice and that the pharmacological inhibition of CtsB prevents *in vitro* HSC activation and proliferation. Consequently, ASMase-knock-out mice exhibit increased *in vivo* liver fibrosis induced by CCl₄ challenge, which is reduced upon CtsB inhibition. Similar findings regarding enhanced basal levels and increased processing of CtsB/D were observed in brain and lung from ASMase-knock-out mice. Thus, these findings imply that the therapeutic targeting of CtsB may be of relevance in the treatment of liver fibrosis in patients with NPD.

EXPERIMENTAL PROCEDURES

Reagents—DMEM, trypsin-EDTA, penicillin-streptomycin, TRIZol, FBS, HistoGrip, and Opti-MEM, were from Invitrogen. All tissue cultureware was from Nunc. The DAKO Biotin Blocking System, peroxidase substrate (DAB), peroxidase buffer, and hematoxylin were from DAKO (Glostrup, Denmark). Aquatex was from Merck. The Vectastain ABC kit was from Vector Laboratories (Burlingame, CA). PDGF-BB was from PeProtechEC (London, UK). Proteinase inhibitors were from Roche Applied Science. iScript™ One-Step reverse transcription (RT)-PCR kit with SYBR® Green was from Bio-Rad. ECL Western blotting substrate was from Pierce. Ca074Me was from Sigma-Aldrich, and, unless otherwise stated, all other reagents were also from Sigma-Aldrich.

Antibodies—We used the following primary antibodies: rabbit polyclonal anti-cathepsin B (catalog 06-480) and rabbit polyclonal anti-Col1A1 (catalog AB765P) were from Millipore. Goat polyclonal anti-cathepsin D (catalog sc-6486) and mouse monoclonal pan-cathepsin (catalog sc-365614) were from Santa Cruz Biotechnology. Rabbit polyclonal anti- α -SMA (catalog ab5694), rabbit polyclonal anti-myeloperoxidase (catalog ab15484), and rat monoclonal anti-lysosomal associated membrane protein 2 (LAMP2) (catalog ab13524) were from Abcam. mAb anti- α -SMA (catalog A2547), mAb anti- β -actin (catalog A1978), and ECL-peroxidase labeled anti-mouse (catalog

A9044), anti-rabbit (catalog A0545), and anti-goat (catalog A5420) were from Sigma-Aldrich. Anti-rat (catalog 819520) was from Invitrogen. Rabbit polyclonal anti-Hsp70 was from Enzo LifeSciences, Farmingdale, NY). Rabbit polyclonal anti-LC3B (catalog 2775) was from Cell Signaling Technology. Alexa Fluor 488 goat anti-rat (catalog A11006), Alexa Fluor 594 rabbit anti-goat (catalog A11080), and Alexa Fluor 647 goat anti-rabbit (catalog A21245) were from Invitrogen. Biotinylated labeled anti-rabbit was from BD Biosciences.

Animals and HSC Isolation—Wild-type and ASMase-knock-out mice (male, 8–10-week-old littermates) (C57BL/6 strain) were obtained by propagation of heterozygous breeding pairs (a generous gift from R. Kolesnick, Memorial Sloan-Kettering Cancer Center, New York and E. Gulbins, University of Duisburg-Essen, Germany) and genotyped as described previously (22). All animals received humane care according to the criteria outlined in the *Guide for the Care and Use of Laboratory Animals* published by the National Institutes of Health. HSCs were isolated by perfusion with collagenase-Pronase and cultured as described previously (10). Culture purity, assessed routinely by retinoid autofluorescence at 350 nm, was >95%. Lack of staining for F4/80 confirmed the absence of Kupffer cells. Cells were cultured in DMEM supplemented with 10% FBS and antibiotics at 37 °C in a humidified atmosphere of 95% air and 5% CO₂.

In Vivo Liver Fibrogenesis—Wild-type or ASMase KO mice were treated with CCl₄ at a dose of 5 μ l (10% CCl₄ in corn oil)/g of body weight, by intraperitoneal injection twice a week for 4 weeks. Control animals received corn oil alone. Ca074Me (Sigma-Aldrich) was administered 30 min before CCl₄ for the last 3 week of the study. Ca074Me was given intraperitoneally in a dosage according to CtsB expression in liver (0.25–1.0 mg/mouse).

ASMase Activity—ASMase activity from cellular extracts was determined using a fluorescent sphingomyelin analog (NBD C6-sphingomyelin). Samples were incubated for 60 min at 37 °C in incubation buffer containing 10 μ mol/liter NBD C6-sphingomyelin (250 mmol/liter sodium acetate, 0.1% Triton X-100, pH 5.0). Lipids were extracted, dried under N₂, and separated by TLC (chloroform:ethanol: 20% NH₄OH; 70:30:5, v/v). NBD-ceramide was visualized under UV light, and images were acquired and analyzed using a Gel Doc XR System with Quantity One software (Bio-Rad). Furthermore, ASMase activity in tissue lysates was performed as described (17).

CtsB and CtsD Activities—CtsB activity was assayed fluorometrically with Z-Arg-Arg-7-amido-4-methylcoumarin hydrochloride (60 μ mol/liter) at pH 7.4 and 37 °C as described previously (10). CtsD was assayed using a Cathepsin D Activity Assay kit (catalog ab65302; Abcam) following the manufacturer's instructions. Results were expressed as cathepsin activity (slope of fluorescence emission after 40 min) per milligram of protein.

SDS-PAGE and Immunoblot Analysis—Cell lysates were prepared in radioimmune precipitation assay buffer (50 mmol/liter Tris-HCl, pH 8, 150 mmol/liter NaCl, 1% Nonidet P-40, 0.1% SDS, 1% Triton X-100 plus proteinase inhibitors). Protein concentration was determined by the Bradford assay, and samples containing 10–30 μ g were separated by 8–10% SDS-PAGE.

Cathepsin B Overexpression in Niemann-Pick Disease

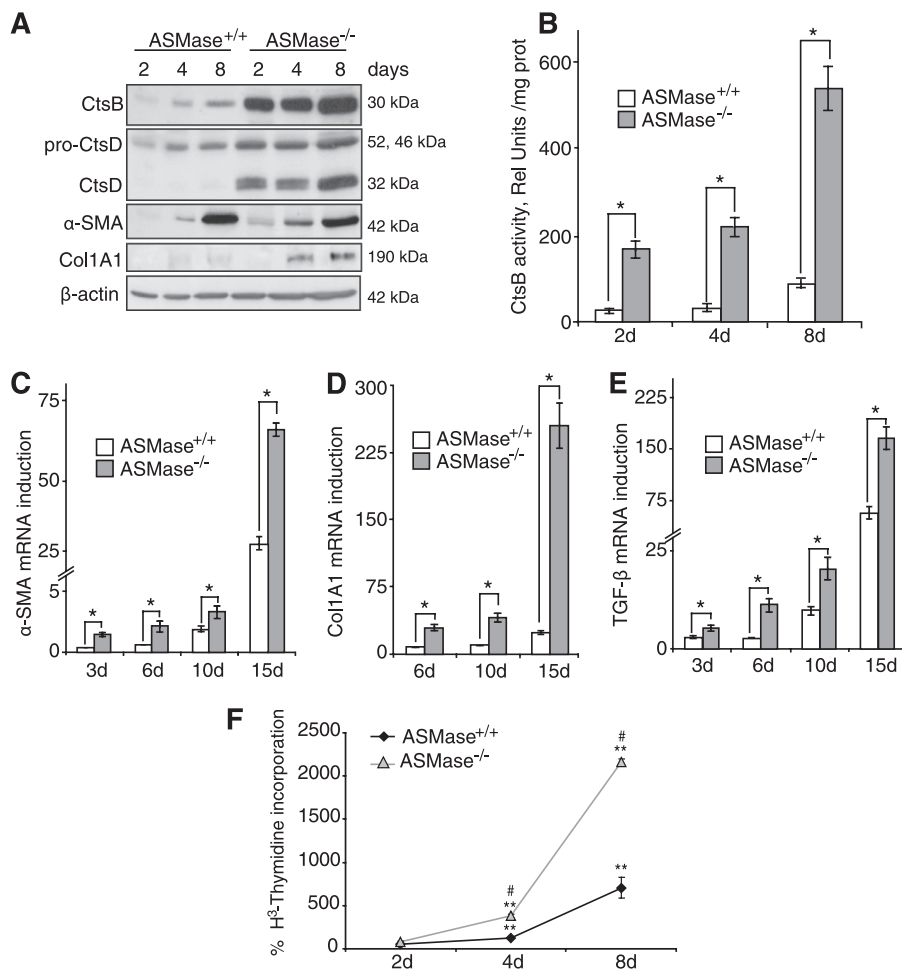


FIGURE 1. Enhanced fibrogenic potential of ASMase^{-/-} HSC. *A*, time course of CtsB, CtsD, α -SMA, and Col1A1 protein expression. *B*, time course of CtsB activity in ASMase^{+/+} and ASMase^{-/-} HSCs. *C–E*, time course of α -SMA (*C*), Col1A1 (*D*), and TGF- β (*E*) mRNA levels in ASMase^{-/-} HSCs compared with ASMase^{+/+} HSCs. *F*, percentage of proliferation from day 2 to day 8 of culture in ASMase^{+/+} and ASMase^{-/-} HSCs. Data are mean \pm S.D. (error bars), $n = 4$. *, $p \leq 0.01$ versus same time point ASMase^{+/+} HSCs; **, $p \leq 0.05$ versus control day 2 HSCs; #, $p \leq 0.05$ versus ASMase^{+/+} HSCs.

Proteins were transferred to nitrocellulose membranes. After membranes were blocked in 8% nonfat milk or 5% BSA in 20 mmol/liter Tris-HCl, 150 mmol/liter NaCl, and 0.05% Tween 20 for 1 h at room temperature, the membranes were incubated overnight at 4 °C with different primary antibodies and developed with the ECL-peroxidase system.

HSC Proliferation—Proliferation was estimated as the amount of [³H]thymidine incorporated into TCA-precipitable material as described previously (17).

Hydroxyproline Content—Hepatic hydroxyproline content was determined by the method of Jamall *et al.* (23), as described previously (10). Data were normalized to wet liver weight.

RNA Isolation and Real Time RT-PCR of Mouse Samples—Total RNA was isolated from HSCs with TRIzol reagent. Real-time RT-PCR was performed with an iScript™ One-Step reverse transcription-PCR kit with SYBR® Green following the manufacturer's instructions. The primers sequences used were: mouse α -SMA forward, 5'-ACTACTGCCGAGCGTGAGAT-3' and reverse, 5'-AAGGTAGACAGCGAAGCCAA-3' (GenBank accession number NM_007392); mouse TGF- β forward, 5'-GTCAGACATTCCGGAAGCAG-3' and reverse, 5'-GCGTATCAGTGGGGTCA-3' (GenBank accession number NM_011577); mouse Col1A1 forward, 5'-ACTTCACTTCC-

TGCCTCAG-3' and reverse, 5'-TGACTCAGGCTCTTGAGGGT-3' (GenBank accession number NM_007742); mouse β -actin forward, 5'-GACGGCCAGGTCATCACTAT-3' and reverse, 5'-CGGATGTCAACGTCACACTT-3' (GenBank accession number NM_007393).

Immunohistochemical Staining—Paraffin molds containing liver sections were cut into 5- μ m sections and mounted on HistoGrip-coated slides. The sections were deparaffinized in xylene and dehydrated in graded alcohol series. Endogenous peroxidase (3% H₂O₂) and avidin and biotin were blocked. Slides were incubated with primary antibody overnight in a wet chamber at 4 °C. After rinsing with PBS 1 \times , the slides were incubated with a biotinylated antibody for 45 min in a wet chamber and developed with the ABC kit with peroxidase substrate (DAB) and peroxidase buffer. After rinsing the slides with tap water they were counterstained with hematoxylin and mounted with Aquatex.

H&E and Sirius Red Staining—Livers were fixed, included in paraffin, and sections of 7 μ m were routinely stained with H&E, periodic acid-Schiff, Nissl staining, or with a 0.1% Sirius Red-picric solution following standard procedures.

Statistical Analyses—All images display representative data from at least three independent observations. The experiments

were repeated at least three times. The statistical significance of differences was performed using the unpaired, nonparametric Student's *t* test.

RESULTS

HSCs from ASMase Knock-out Mice Exhibit Increased CtsB/D Processing and Fibrogenic Potential—Given the functional relationship between ASMase and cathepsins recently reported in liver fibrosis (17), we analyzed the expression of CtsB and CtsD in HSCs from ASMase^{-/-} mice. HSCs were isolated and cultured in plastic to follow their activation process *in vitro* from quiescent HSCs to myofibroblasts like cells responsible for the fiber deposition. As shown in Fig. 1A we observed an up-regulation of CtsB and CtsD expression and processing compared with wild-type HSCs. In particular, CtsB expression was remarkably induced, as shown by the enhanced activity of CtsB in ASMase^{-/-} HSCs compared with wild-type HSCs (Fig. 1B). Kinetic analyses revealed enhanced expression of CtsB/D at the early phase in the activation of HSC (Fig. 1, A and B). Genetic deficiency of ASMase also resulted in elevated expression of the activation markers α -SMA and Col1A1 at the protein (Fig. 1A) and mRNA level (Fig. 1, C and D), which was further accompanied by overexpression of other markers of HSC activation such as transforming growth factor- β (TGF- β) (Fig. 1E). Considering the difference in -fold increase of mRNA levels for α -SMA and Col1A1, the corresponding increase at the protein level at day 8 of culture was more apparent for Col1A1 than for α -SMA. In parallel with these observations, the proliferation rate of HSC from day 2 after isolation to day 8 of culture was significantly increased in ASMase^{-/-} HSCs compared with wild-type HSCs (Fig. 1F). Thus, HSCs from ASMase^{-/-} mice exhibit increased fibrogenic potential, which correlated with enhanced CtsB/D levels and processing.

CtsB Inhibition Diminishes Activation of ASMase-knock-out HSCs—According to our observations in the knock-out mice, complete absence of ASMase up-regulates CtsB and CtsD. Because in previous studies we have already disclosed the importance of CtsB in liver fibrosis and that the use of a selective CtsB inhibitor (Ca074Me) reduced HSC activation in an experimental liver fibrosis model (10), we decided to test whether the up-regulation of CtsB observed in ASMase^{-/-} HSCs plays a causal role in their enhanced fibrogenic potential, evaluating the effect of inhibiting CtsB using the specific inhibitor Ca074Me. In analyzing the expression of α -SMA and Col1A1 in 7-day-old HSC cultures, we observed an increased expression of these markers of HSC transdifferentiation that was prevented after Ca074Me treatment, both in wild-type and ASMase^{-/-} HSCs (Fig. 2A). Moreover, proliferation was also significantly diminished under these conditions, even in ASMase^{-/-} HSCs (Fig. 2B). As previously observed in wild-type HSCs (10), AKT phosphorylation induced by PDGF was enhanced in HSC from ASMase-knock-out mice and blocked by Ca074Me (data not shown). Ca074Me did not cause any noticeable cell death or toxicity at the doses and time utilized. Hence, these results suggest that CtsB is responsible for the enhanced fibrogenic features observed in ASMase-knock-out HSCs.

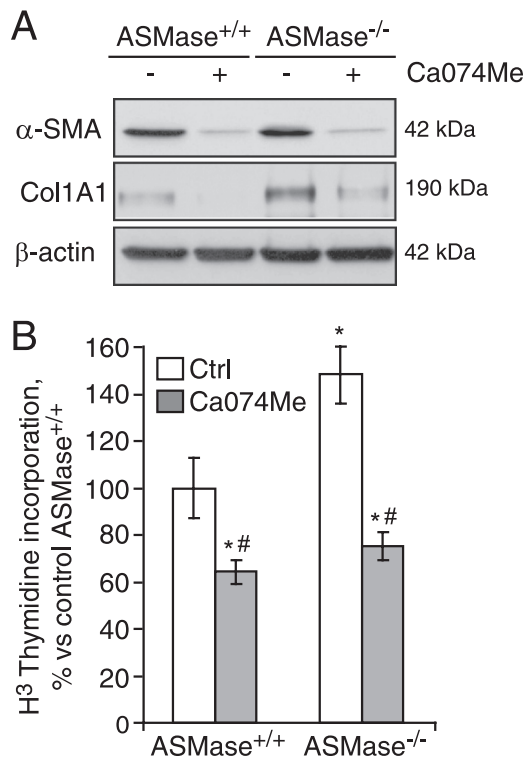


FIGURE 2. CtsB inhibition decreases the fibrogenic potential of HSCs. A, α -SMA and Col1A1 protein levels, and B, proliferation rate after CtsB inhibition with Ca074Me (20 μ mol/liter, 48 h, added every 24 h from day 5 to day 7), in ASMase^{+/+} and ASMase^{-/-} HSCs. Data are mean \pm S.D. (error bars), *n* = 3. *, *p* \leq 0.05 versus ASMase^{+/+} control HSC; #, *p* \leq 0.05 versus respective controls.

ASMase-knock-out Mice Exhibit Increased Liver Fibrosis in Response to CCl₄ Due to CtsB Overexpression—Our previous studies indicated that heterozygous ASMase mice are less sensitive to *in vivo* liver fibrosis due to impaired CtsB activation. However, the preceding findings indicate that the complete loss of ASMase leads to increased CtsB expression, which is known to contribute to liver fibrosis and is a marker of disease progression in NASH patients (17). Therefore, to analyze whether CtsB overexpression sensitizes to liver fibrosis we decided to administer CCl₄ to ASMase^{-/-} and wild-type mice. We chose CCl₄ instead of bile duct ligation because the degree of liver damage is independent of ASMase (17). CCl₄ challenge for 4 weeks increased serum alanine transaminase levels in wild-type and ASMase deficient mice to a similar extent (Fig. 3A). As shown in Fig. 3B, basal levels of CtsB activity were increased in ASMase^{-/-} livers and were further enhanced upon induction of liver fibrosis with CCl₄ only in ASMase-deficient livers. In addition, enhanced levels of CtsD were also detected in ASMase-deficient livers that were further increased after CCl₄ challenge (Fig. 3C). Moreover, in CCl₄-treated animals enhanced levels of CtsB and CtsD correlated with an elevated α -SMA expression, as shown by Western blot analysis (Fig. 3C) and immunohistochemistry (Fig. 3E), indicating that ASMase-deficient animals have increased number of activated HSCs. Analysis of the hydroxyproline content in the liver revealed a significant increase in collagen accumulation in ASMase-deficient animals compared with wild-type animals after CCl₄ administration (Fig. 3D), which correlated with the increased

Cathepsin B Overexpression in Niemann-Pick Disease

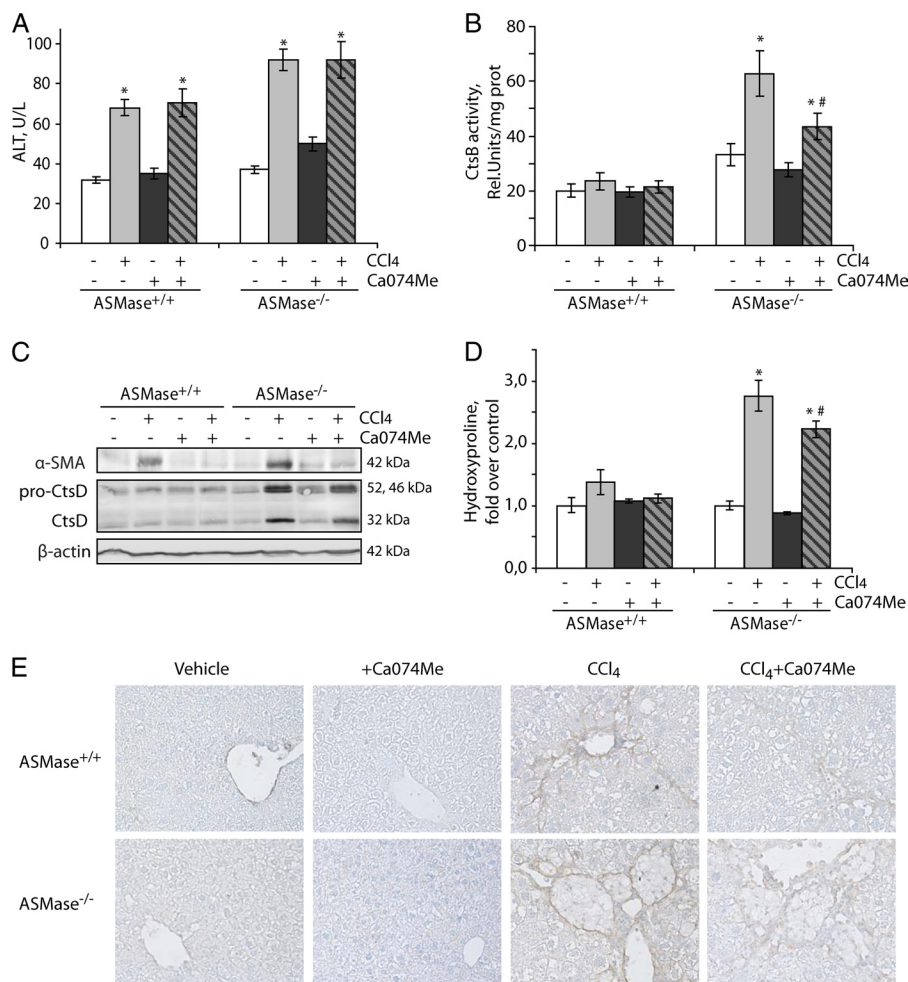


FIGURE 3. Enhanced liver fibrosis in ASMase^{-/-} mice after CCl₄ administration was ameliorated after CtsB inhibition. A–D, serum alanine transaminase (ALT) levels (A), CtsB activity (B), CtsD and α -SMA protein expression (C), and hydroxyproline levels in liver homogenate (D). E, α -SMA immunostaining of liver section at $\times 40$ magnification. Data are mean \pm S.E. (error bars), $n = 6$ animals/group. *, $p \leq 0.05$ versus vehicle-treated mice; #, $p \leq 0.05$ versus CCl₄ ASMase^{-/-}-treated mice.

detection of collagen fibers in the livers of ASMase^{-/-} mice that received CCl₄, as detected by Sirius Red staining (Fig. 4A). The Sirius Red staining, as well as the α -SMA expression, observed in the ASMase^{-/-} livers did not follow the typical pattern along the collagen fibers but displayed a characteristic arrangement surrounding foam cells, lipid-accumulating macrophages also known as Niemann-Pick cells. This atypical distribution was observed only in ASMase-deficient livers that received CCl₄; this particular cell type, however, was not observed in ASMase^{-/-} animals receiving only vehicle (Fig. 4A). On histological examination we observed mild sinusoidal dilatation, by H&E staining (Fig. 4B), and moderate neutrophilic infiltration, as detected by myeloperoxidase immunostaining (Fig. 4C) in wild-type livers upon CCl₄ challenge. These parameters were exacerbated in ASMase^{-/-} animals that presented noticeable infiltration of neutrophils especially adjacent to foam cells, clearly visible by H&E staining. Collectively, these results indicate that liver fibrosis is significantly increased in ASMase-KO mice.

CtsB Inhibition Reduces *In Vivo* Liver Fibrosis in ASMase-null Mice—Given the above findings, and because CtsB inhibition has been proven useful in reversing liver fibrosis in wild-type

mice (10), we next asked whether CtsB inhibition could be of relevance in ameliorating liver fibrogenesis in ASMase^{-/-} livers *in vivo* following CCl₄ administration. To this aim, CCl₄ was first administered twice a week for 1 week, followed by CCl₄ and Ca074Me administration for 3 additional weeks. CtsB inhibition by itself did not alter any of the parameters studied in control animals (Figs. 3 and 4). As described previously (10), Ca074Me treatment did not significantly affect the increase in alanine transaminase levels observed after CCl₄ challenge, suggesting that CtsB did not participate in the mechanisms responsible for liver damage (Fig. 3A). However, *in vivo* Ca074Me administration significantly reduced the increase in CtsB activity (~30%) induced by CCl₄ in ASMase^{-/-} mice (Fig. 3B). Higher doses of Ca074Me failed to inhibit CtsB activity in ASMase^{-/-} mice further (data not shown). CtsB inhibition by Ca074Me reduced the increased expression of α -SMA and CtsD (Fig. 3C) as well as the presence of α -SMA-positive cells after CCl₄ challenge in ASMase^{-/-} livers (Fig. 3D). Moreover, as shown in Fig. 3E, determination of the hydroxyproline content in the liver revealed a significant decrease in collagen accumulation in CCl₄-treated mice that received Ca074Me, compared with mice challenged with CCl₄ alone. This result was

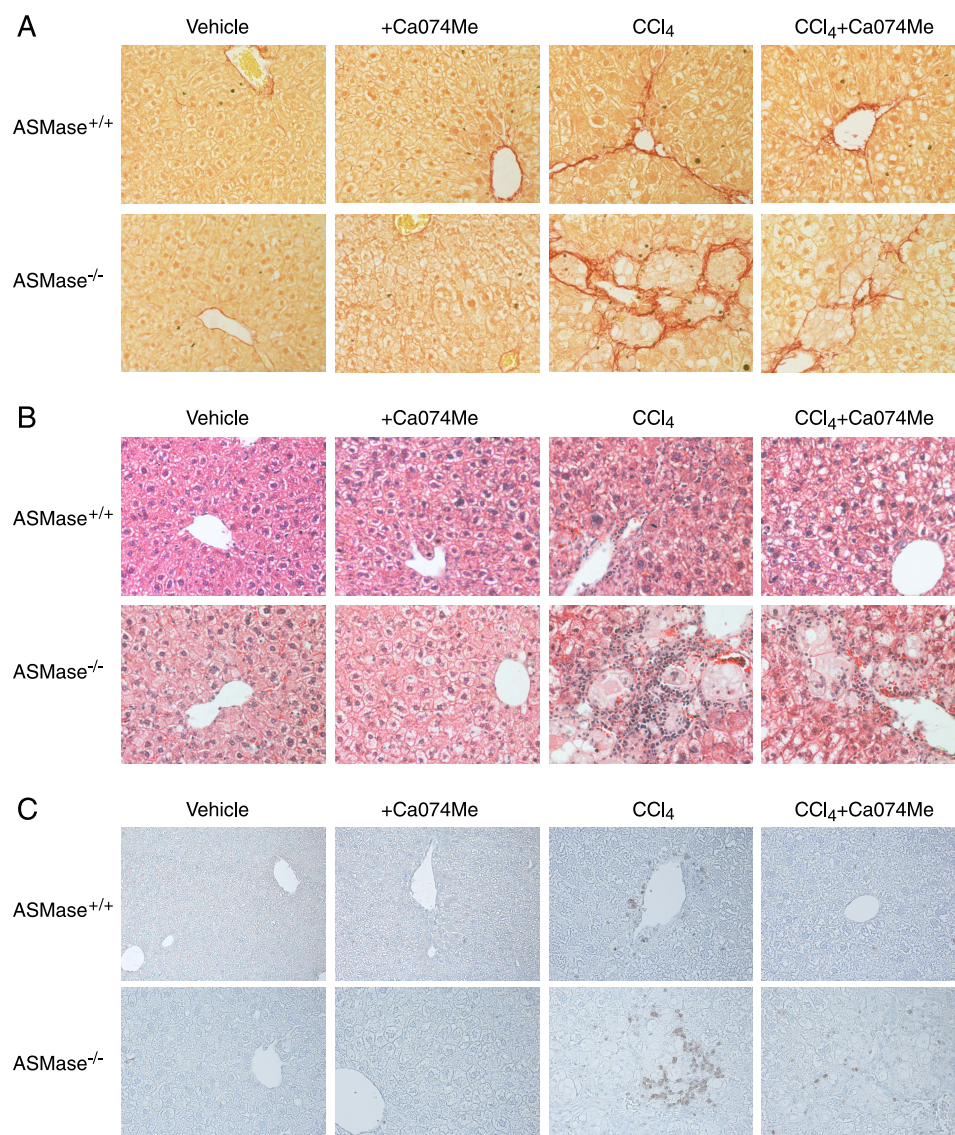


FIGURE 4. **Fiber deposition, presence of foam cells, and inflammation were decreased in ASMase^{-/-} livers after CtsB inhibition.** A, Sirius Red staining of collagen fibers. B and C, H&E (B) and myeloperoxidase (C) staining of liver sections after the corresponding treatments. All images were taken at $\times 40$ magnification.

further confirmed by the detection of collagen fibers by Sirius Red staining (Fig. 4A) in CCl₄-treated animals compared with those treated with CtsB inhibitor. Additionally, CtsB inhibition in CCl₄-treated animals moderately decreased the incidence of foam cells in the liver (Fig. 4B) and the number of myeloperoxidase-positive cells (Fig. 4C). Thus, these findings indicate that CtsB plays a critical role in *in vivo* liver fibrogenesis in ASMase-deficient livers.

CtsB and D Increase in Extrahepatic Organs in ASMase-knock-out Mice—To analyze whether the increase of CtsB and CtsD was an isolated feature of the liver from the ASMase^{-/-} mice or was a general phenotypic characteristic in other organs, 21-week-old animals were killed, and different organs were harvested. CtsB (Fig. 5A) and CtsD (Fig. 5B) protein expression and activity increased in several organs affected by the accumulation of foam cells in NPD: brain, lung, liver, muscle, epididymal white adipose tissue (EWAT), and skin. However, there were no changes in spleen, pancreas, and intestine in those mice. When

exploring the magnitude of ASMase and CtsB activities in the tissues of wild-type animals we did not observe any direct correlation between the extent of activation of these two enzymes in view of the fact that tissues with the lowest ASMase activity, such as spleen and muscle, displayed, respectively, the highest and the lowest CtsB activities among the tissues examined (Fig. 5C).

To analyze whether the increase in CtsB was also detectable in younger animals with a weak NPD phenotype, 10–12-week-old mice were studied. Accumulation of foam cells was already detectable in histological sections of lung and liver, as well as a decrease in the number of Purkinje cells in the cerebellum (Fig. 6A), both characteristic of the neurovisceral phenotype of the NPD. No changes were appreciated in spleen sections (data not shown). Interestingly, when enzymatic activity was measured in these almost asymptomatic young animals, CtsB was already significantly increased in the lung and liver tissue from the ASMase-knock-out mice (Fig. 6B), even

Cathepsin B Overexpression in Niemann-Pick Disease

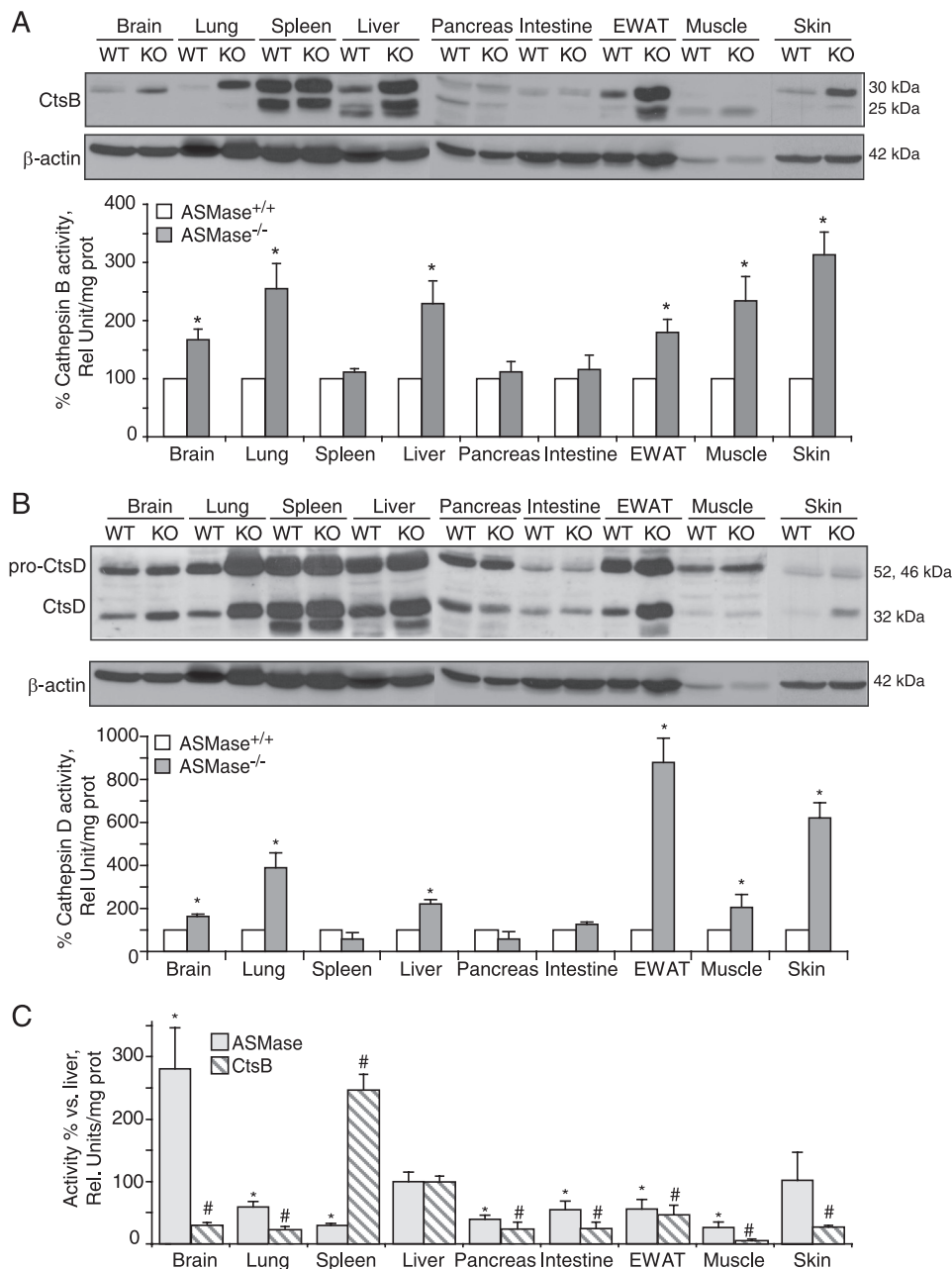


FIGURE 5. CtsB and CtsD increase in the organs affected by the NPD phenotype. A and B, CtsB (A) and CtsD (B) protein expression and activity in total lysates of brain, lung, spleen, liver, pancreas, intestine, EWAT, muscle, and skin of 21-week-old $ASMase^{-/-}$ and $ASMase^{+/+}$ mice. C, ASMase and CtsB activities in the same tissues of $ASMase^{+/+}$ mice. In A and B, data are mean \pm S.D. (error bars), $n = 6$; *, $p \leq 0.05$ versus $ASMase^{+/+}$. In C, $n = 4$; *, $p \leq 0.05$ versus ASMase activity in liver; #, $p \leq 0.05$ versus CtsB activity in liver of $ASMase^{+/+}$ mice.

despite the weak accumulation of foam cells in these tissues, which represents an early feature of the NPD phenotype. In contrast, no changes in CtsB activity were detected in brain and spleen at this age.

Role of Other Cathepsins, Lysosomal Stability, and Autophagy—To address the potential participation of other cathepsins in the NPD phenotype, we used a pan-cathepsin antibody with specificity toward several cathepsins other than CtsB/CtsD. As seen (Fig. 7A) the pattern of pan-cathepsin expression between $ASMase^{+/+}$ and $ASMase^{-/-}$ HSCs was similar. Moreover, although there were different patterns of expression among tissues, there were no major differences between $ASMase^{+/+}$ and $ASMase^{-/-}$ mice (Fig. 7B), except the observed enhanced pan-

cathepsin expression in lung from $ASMase^{-/-}$ mice. Consequently, it is feasible that the participation of other cathepsins in NPD phenotype may be tissue-specific.

Given that an increase in cathepsins in the lysosome can lead to lysosomal membrane permeabilization and subsequent release of cathepsins leading to apoptosis (24), we next analyzed whether lysosomal stability was affected and whether CtsB and CtsD were localized in the lysosomes of $ASMase^{-/-}$ HSC. As shown in Fig. 7A, LAMP2 expression, known to correlate with lysosomal stability (25), was increased during HSC activation in $ASMase^{-/-}$ HSCs compared with $ASMase^{+/+}$ HSCs at all time points analyzed, suggesting that in addition to increased CtsB and CtsD expression there seems to be enhanced lysosomal

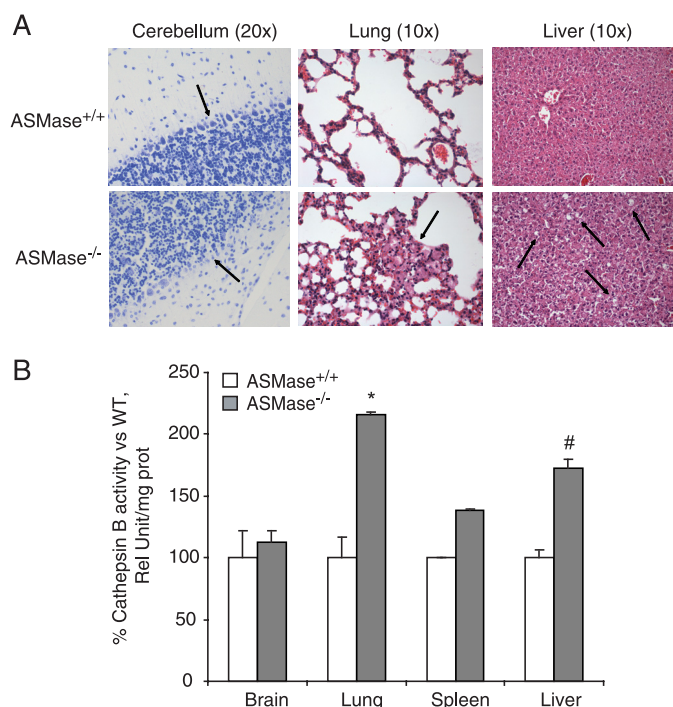


FIGURE 6. CtsB is increased in 10–12-week-old animals with weak NPD phenotype. *A*, Nissl staining in cerebellum histological sections and H&E staining of lung and liver sections. The *arrows* indicate the Purkinje cell population in cerebellum, population decreased in ASMase^{-/-} mice, and the presence of foam cells in lung and liver in ASMase^{-/-} mice. *B*, CtsB activity in total lysates of brain, lung, spleen, and liver of 10–12-week-old ASMase^{-/-} and ASMase^{+/+} mice. Data are mean \pm S.D. (error bars), $n = 3$; *, $p \leq 0.01$ versus ASMase^{+/+}; #, $p \leq 0.05$ versus ASMase^{+/+}.

mass. LAMP2 expression was also enhanced in various tissues of ASMase^{-/-} mice, particularly lung, liver, and spleen (Fig. 7B). In agreement with these findings, immunofluorescence analyses of HSCs from wild-type and ASMase-null mice indicated co-localization of both CtsB and CtsD with LAMP2, a lysosomal marker (Fig. 7C) and revealed increased LAMP2 staining in ASMase^{-/-} HSCs compared with ASMase^{+/+} HSCs. However, no increase was observed in the expression of Hsp70, a chaperone known to facilitate ASMase activity and stabilize lysosomes (26), neither in HSCs (Fig. 7A) nor in the different tissues analyzed (Fig. 7B). Thus, these findings suggest that the increased CtsB expression in ASMase^{-/-} HSCs may be due to lysosomal enlargement.

Because autophagy is a catabolic process involving the degradation of cellular constituents through lysosomal digestion, we asked whether it played a role in HSC activation and tissue degeneration in NPD. To address this point, we monitored LC3 expression in the different tissues of wild-type and ASMase^{-/-} mice. As shown in Fig. 7B, the amount of LC3-I varied among tissues but remained constant between ASMase^{+/+} and ASMase^{-/-} animals. There was, however, more expression of LC3-II in lung, intestine, EWAT, and skin of ASMase^{-/-} mice compared with ASMase^{+/+} mice. In addition, no expression of LC3-II was observed during HSC activation (Fig. 7A). Therefore, no direct relationship was found between CtsB or CtsD expression (Fig. 5) and LC3-I conversion to LC3-II in the NPD mouse model.

DISCUSSION

NPD is a rare lysosomal disorder caused by the loss of ASMase. Patients with NPD exhibit neurodegeneration, lung dysfunction, hepatosplenomegaly, and liver disease. Although all lysosomal storage diseases are characterized by the intralysosomal accumulation of unmetabolized substrates, acting as a primary cause of the disease, the extensive range of disease symptoms indicates that many secondary biochemical and cellular pathways can contribute to the plethora of phenotypes reported (27). Currently, there is no treatment for NPD patients, and the degree of pathology depends on the extent of ASMase loss. In the present study we extend our initial observations between ASMase and CtsB/D in HSC and liver fibrosis, which occurs in a large percentage of NPD patients (6). Heterozygous ASMase mice, which exhibit a residual 30–40% ASMase activity, are protected against *in vivo* liver fibrosis due to a decreased CtsB/D activation (17). Moreover, pharmacological ASMase inhibition (by 70–80%) decreased CtsB/D activation and the fibrogenic potential and proliferation of murine and human HSC. Quite surprisingly, we observe here that the genetic ablation of ASMase leads to a paradoxical increased basal level and activity of CtsB, which confers increased fibrogenic potential and proliferation on HSCs from ASMase-null mice leading to enhanced liver fibrosis.

Consistent with findings in death ligand-induced apoptosis (15), our previous studies disclosed a hierarchical functional relationship between ASMase and CtsB of relevance in liver fibrosis (17). Unlike the pharmacological inhibition of ASMase, which impaired CtsB/D maturation and hence HSC activation, the inhibition of CtsB did not affect ASMase activity during *in vitro* HSC activation, indicating that ASMase is required for and upstream of CtsB/D proteolytic processing and that the gradual down-regulation of ASMase, as in the heterozygous ASMase mice, results in impaired CtsB/D processing and activation. Although genetic CtsD silencing did reduce HSC proliferation and α -SMA expression in line with the effects observed with CtsB silencing, it did not affect HSC migration (10). Moreover, unlike CtsD, the expression of CtsB appears to be more restricted to activated HSC (10), suggesting that CtsB rather than CtsD may be a better target to address its role in liver fibrosis in NPD (10). Although the present findings support a critical role for CtsB in hepatic fibrosis in NPD, we cannot rule out a potential contribution of other cathepsins, including CtsD.

Due to the critical role of CtsB in liver fibrosis (10), the proportional direct relationship between the down-regulation of ASMase and CtsB dictates a low susceptibility of the ASMase^{+/+} mice to liver fibrosis (17). However, unexpectedly, the loss of ASMase below a critical threshold toward the total deficiency of ASMase, as in the ASMase-knock-out mice, results in an adaptive increase in the basal levels of some cathepsins and enhanced proteolytic processing during HSC activation *in vitro* that sensitizes ASMase-null mice to *in vivo* fibrosis. The unexpected rebound relationship between the loss of ASMase and activation of CtsB may be of particular relevance to type A but not type B NPD patients, which exhibit a residual ASMase activity. Pharmacological inhibition of CtsB decreases

Cathepsin B Overexpression in Niemann-Pick Disease

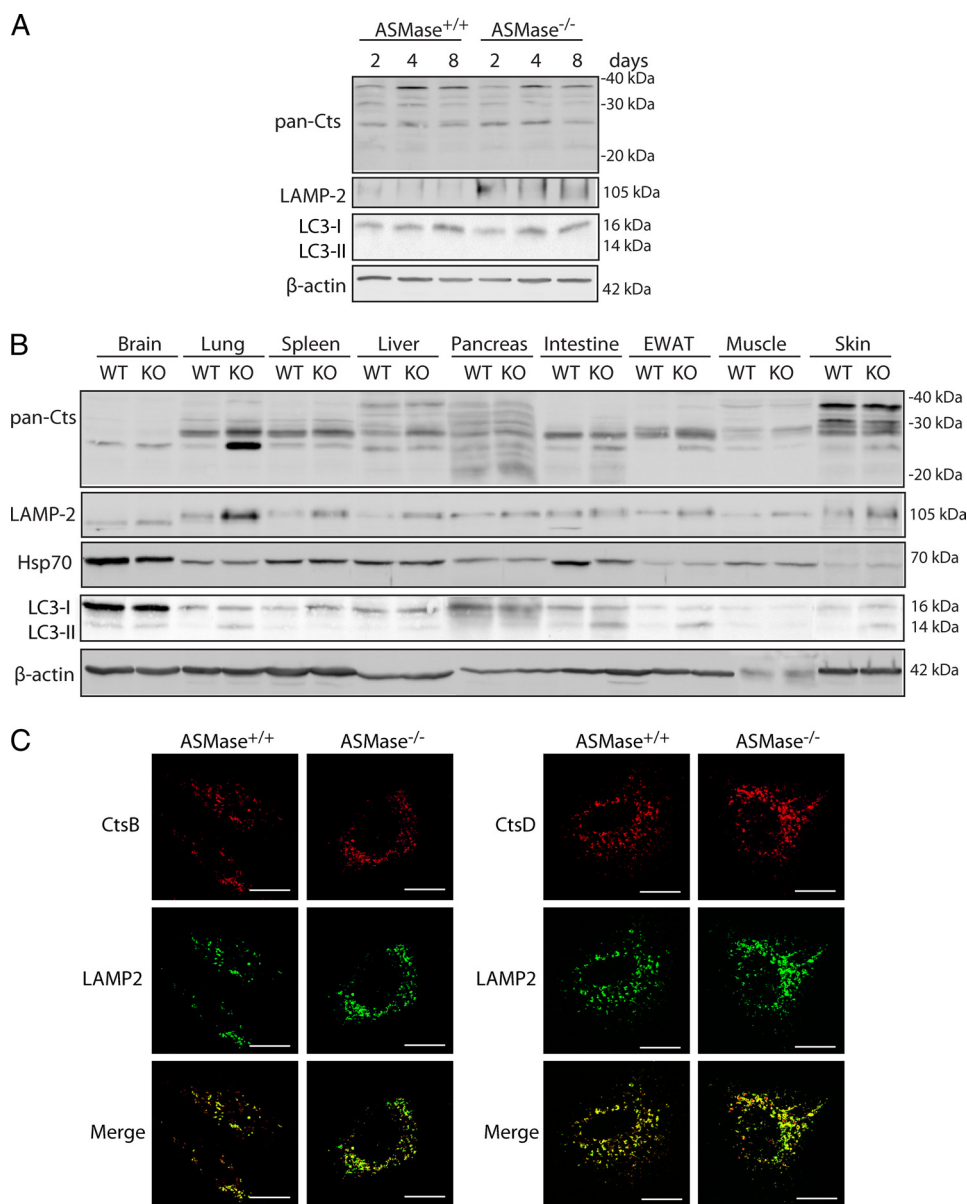


FIGURE 7. Analysis of other cathepsins, lysosomal stability, and autophagy in the NPD mouse model. *A*, time course of pan-cathepsin, LAMP2, and LC3 expression in ASMase^{+/+} and ASMase^{-/-} HSCs. *B*, pan-cathepsin, LAMP2, Hsp70, and LC3 expression in total lysates of brain, lung, spleen, liver, pancreas, intestine, EWAT, muscle, and skin of 21-weeks old ASMase^{-/-} and ASMase^{+/+} mice. *C*) Confocal imaging of 7 day-old ASMase^{+/+} and ASMase^{-/-} HSCs displaying CtsB and CtsD co-localization with a lysosomal marker (LAMP2). Scale bars, 10 μm.

the *in vitro* activation of HSC from ASMase-null mice and *in vivo* liver fibrosis, thus suggesting that targeting CtsB may be a novel treatment for the underlying liver fibrosis in NPD patients.

Similar to the NPD phenotype, patients with Niemann-Pick type C1 (NPC1) disease caused by mutation in NPC1, an endosomal/lysosomal protein that regulates intracellular cholesterol trafficking, exhibit similar biochemical changes including free cholesterol, sphingolipids, and bis-(monoacylglycerol) phosphate accumulation in intracellular compartments, including lysosomes and mitochondria from affected organs including brain and liver (28, 29). Interestingly, similar to the findings presented in the current study, Amritraj *et al.* described increased CtsB/D activity in neurons from the cerebellum of NPC1^{-/-} mouse brain (30). Consistent with the lack of neuro-

nal degeneration in the hippocampus of NPC1^{-/-} mouse, CtsB activation was not observed in this particular neuron population, thus establishing a correlation between increased CtsB activity and selective neurological dysfunction in NPC1 disease. Our findings indicate that CtsB and CtsD enhanced expression in the ASMase^{-/-} mice are accompanied by an increase in lysosomal mass, but are probably not related to autophagy. Of note, although Hsp70 has been found to correlate not only with lysosomal stability but also to reverse NPD associated lysosomal pathology (31), we did not observe up-regulation of Hsp70 in ASMase^{-/-} tissues. In line with our observations, studies in fibroblasts of NPC1 patients or after treatment of normal fibroblasts with U18666A, a drug that reproduces the NPC1 phenotype by increasing free cholesterol accumulation in lysosomes, indicate that enhanced lysosomal cholesterol

stimulates CtsD and LAMP2 expression, resulting in increased lysosomal stability and resistance to apoptosis (32). Moreover, these results were also independent of Hsp70 expression or autophagy. Of interest, secondary to ASMase deficiency there may be several associated changes in different tissues of ASMase-null mice, including sphingolipids and cholesterol (33). However, unlike these data reported in 5-month-old ASMase-null mice, our findings did not reveal any change in the hepatic cholesterol levels in 8–10-week-old ASMase-knock-out mice (data not shown), suggesting that the increase of hepatic cholesterol in the NPD mouse model may be age-related and that cholesterol plays a minor role in the increased susceptibility of ASMase-null mice to hepatic fibrosis. Moreover, the protection against liver fibrosis afforded after CtsB inhibition appears to be independent on cholesterol changes.

Our findings imply that liver fibrosis of NPD type A patients could be corrected by targeting a secondary associated enzyme, namely that the genetic cause of NPD type A liver disease due to the lack of ASMase, can be overcome by the inhibition of the adaptive increase in CtsB processing. Consistent with this concept, it has been shown that the phenotype defects observed in NPC1 disease, including free cholesterol accumulation and impaired transferring receptor recycling, could be corrected by overexpressing ASMase, whose expression is also decreased in NPC1 disease (34).

An important feature of the present study is that the up-regulation of CtsB due to the lack of ASMase is not restricted to liver, but also observed in other affected organs, such as brain and lung, in an age-dependent mechanism. Of relevance to the neurological phenotype, there seems to be a threshold for ASMase activity below which these symptoms arise. For instance, it has been shown using mutation-specific mouse models that as little as 8% ASMase activity can completely prevent the occurrence of neurological disease (35). In addition, whereas the residual ASMase activity of ~5% results in NPD type B, a further reduction to ~1–2% or less induces the severe type A phenotype (36). These observations highlight the fact that although low levels of ASMase activity are sufficient to maintain intact neurological function, the absence of this activity has devastating consequences in the brain (37).

Collectively, our results point to a new role for ASMase-CtsB axis in NPD. In addition to its known function as a proapoptotic intermediate in TNF- or Fas-induced cell death (15, 38), ASMase plays a critical role in regulating cathepsin processing and hence in modulating the diverse phenotypes of NPD, including liver disease and neurological manifestations of the disease. Thus, targeting the increase in CtsB secondary to the loss of ASMase may be of relevance to NPD, particularly for the fibrosis and liver disease phenotype of the disease.

Acknowledgment—We thank Susana Núñez for technical assistance.

REFERENCES

- Jenkins, R. W., Canals, D., and Hannun, Y. A. (2009) Roles and regulation of secretory and lysosomal acid sphingomyelinase. *Cell. Signal.* **21**, 836–846
- Morales, A., Lee, H., Goñi, F. M., Kolesnick, R., and Fernandez-Checa, J. C. (2007) Sphingolipids and cell death. *Apoptosis* **12**, 923–939
- Smith, E. L., and Schuchman, E. H. (2008) The unexpected role of acid sphingomyelinase in cell death and the pathophysiology of common diseases. *FASEB J.* **22**, 3419–3431
- Jenkins, R. W., Idkowiak-Baldys, J., Simbari, F., Canals, D., Roddy, P., Riner, C. D., Clarke, C. J., and Hannun, Y. A. (2011) A novel mechanism of lysosomal acid sphingomyelinase maturation: requirement for carboxyl-terminal proteolytic processing. *J. Biol. Chem.* **286**, 3777–3788
- Schneider, P. B., and Kennedy, E. P. (1967) Sphingomyelinase in normal human spleens and in spleens from subjects with Niemann-Pick disease. *J. Lipid Res.* **8**, 202–209
- Schuchman, E. H. (2010) Acid sphingomyelinase, cell membranes and human disease: lessons from Niemann-Pick disease. *FEBS Lett.* **584**, 1895–1900
- Schuchman, E. H. (2009) The pathogenesis and treatment of acid sphingomyelinase-deficient Niemann-Pick disease. *Int. J. Clin. Pharmacol. Ther.* **47**, S48–S57
- Horinouchi, K., Erlich, S., Perl, D. P., Ferlinz, K., Bisgaier, C. L., Sandhoff, K., Desnick, R. J., Stewart, C. L., and Schuchman, E. H. (1995) Acid sphingomyelinase deficient mice: a model of types A and B Niemann-Pick disease. *Nat. Genet.* **10**, 288–293
- Otterbach, B., and Stoffel, W. (1995) Acid sphingomyelinase-deficient mice mimic the neurovisceral form of human lysosomal storage disease (Niemann-Pick disease). *Cell* **81**, 1053–1061
- Moles, A., Tarrats, N., Fernández-Checa, J. C., and Mari, M. (2009) Cathepsins B and D drive hepatic stellate cell proliferation and promote their fibrogenic potential. *Hepatology* **49**, 1297–1307
- Lutgens, S. P., Cleutjens, K. B., Daemen, M. J., and Heeneman, S. (2007) Cathepsin cysteine proteases in cardiovascular disease. *FASEB J.* **21**, 3029–3041
- Haque, A., Banik, N. L., and Ray, S. K. (2008) New insights into the roles of endolysosomal cathepsins in the pathogenesis of Alzheimer's disease: cathepsin inhibitors as potential therapeutics. *CNS Neurol. Disord. Drug Targets* **7**, 270–277
- Vasiljeva, O., Reinheckel, T., Peters, C., Turk, D., Turk, V., and Turk, B. (2007) Emerging roles of cysteine cathepsins in disease and their potential as drug targets. *Curr. Pharm. Des.* **13**, 387–403
- Leto, G., Tumminello, F. M., Pizzolanti, G., Montalto, G., Soresi, M., Ruggeri, I., and Gebbia, N. (1996) Cathepsin D serum mass concentrations in patients with hepatocellular carcinoma and/or liver cirrhosis. *Eur. J. Clin. Chem. Clin. Biochem.* **34**, 555–560
- Heinrich, M., Neumeyer, J., Jakob, M., Hallas, C., Tchikov, V., Winoto-Morbach, S., Wickel, M., Schneider-Brachert, W., Trauzold, A., Hethke, A., and Schütze, S. (2004) Cathepsin D links TNF-induced acid sphingomyelinase to Bid-mediated caspase-9 and -3 activation. *Cell Death Differ.* **11**, 550–563
- Guicciardi, M. E., Deussing, J., Miyoshi, H., Bronk, S. F., Svingen, P. A., Peters, C., Kaufmann, S. H., and Gores, G. J. (2000) Cathepsin B contributes to TNF- α -mediated hepatocyte apoptosis by promoting mitochondrial release of cytochrome c. *J. Clin. Invest.* **106**, 1127–1137
- Moles, A., Tarrats, N., Morales, A., Domínguez, M., Bataller, R., Caballería, J., García-Ruiz, C., Fernández-Checa, J. C., and Mari, M. (2010) Acidic sphingomyelinase controls hepatic stellate cell activation and *in vivo* liver fibrogenesis. *Am. J. Pathol.* **177**, 1214–1224
- Labrune, P., Bedossa, P., Huguet, P., Roset, F., Vanier, M. T., and Odievre, M. (1991) Fatal liver failure in two children with Niemann-Pick disease type B. *J. Pediatr. Gastroenterol. Nutr.* **13**, 104–109
- Tassoni, J. P., Jr., Fawaz, K. A., and Johnston, D. E. (1991) Cirrhosis and portal hypertension in a patient with adult Niemann-Pick disease. *Gastroenterology* **100**, 567–569
- Fotoulaki, M., Schuchman, E. H., Simonaro, C. M., Augoustides-Savvopoulou, P., Michelakakis, H., Panagopoulou, P., Varlamis, G., and Nousia-Arvanitakis, S. (2007) Acid sphingomyelinase-deficient Niemann-Pick disease: novel findings in a Greek child. *J. Inher. Metab. Dis.* **30**, 986
- Takahashi, T., Akiyama, K., Tomihara, M., Tokudome, T., Nishinomiya, F., Tazawa, Y., Horinouchi, K., Sakiyama, T., and Takada, G. (1997) Heterogeneity of liver disorder in type B Niemann-Pick disease. *Hum. Pathol.* **28**, 385–388
- Mari, M., Colell, A., Morales, A., Pañeda, C., Varela-Nieto, I., García-Ruiz,

Cathepsin B Overexpression in Niemann-Pick Disease

- C., and Fernández-Checa, J. C. (2004) Acidic sphingomyelinase down-regulates the liver-specific methionine adenosyltransferase 1A, contributing to tumor necrosis factor-induced lethal hepatitis. *J. Clin. Invest.* **113**, 895–904
23. Jamall, I. S., Finelli, V. N., and Que Hee, S. S. (1981) A simple method to determine nanogram levels of 4-hydroxyproline in biological tissues. *Anal. Biochem.* **112**, 70–75
24. Johansson, A. C., Appelqvist, H., Nilsson, C., Kågedal, K., Roberg, K., and Ollinger, K. (2010) Regulation of apoptosis-associated lysosomal membrane permeabilization. *Apoptosis* **15**, 527–540
25. Fehrenbacher, N., Bastholm, L., Kirkegaard-Sørensen, T., Rafn, B., Bøttzauw, T., Nielsen, C., Weber, E., Shirasawa, S., Kallunki, T., and Jäättelä, M. (2008) Sensitization to the lysosomal cell death pathway by oncogene-induced down-regulation of lysosome-associated membrane proteins 1 and 2. *Cancer Res.* **68**, 6623–6633
26. Petersen, N. H., Kirkegaard, T., Olsen, O. D., and Jäättelä, M. (2010) Connecting Hsp70, sphingolipid metabolism and lysosomal stability. *Cell Cycle* **9**, 2305–2309
27. Futerman, A. H., and van Meer, G. (2004) The cell biology of lysosomal storage disorders. *Nat. Rev. Mol. Cell Biol.* **5**, 554–565
28. Mari, M., Caballero, F., Colell, A., Morales, A., Caballeria, J., Fernandez, A., Enrich, C., Fernandez-Checa, J. C., and García-Ruiz, C. (2006) Mitochondrial free cholesterol loading sensitizes to TNF- and Fas-mediated steatohepatitis. *Cell Metab.* **4**, 185–198
29. Yu, W., Gong, J. S., Ko, M., Garver, W. S., Yanagisawa, K., and Michikawa, M. (2005) Altered cholesterol metabolism in Niemann-Pick type C1 mouse brains affects mitochondrial function. *J. Biol. Chem.* **280**, 11731–11739
30. Amritraj, A., Peake, K., Kodam, A., Salio, C., Merighi, A., Vance, J. E., and Kar, S. (2009) Increased activity and altered subcellular distribution of lysosomal enzymes determine neuronal vulnerability in Niemann-Pick type C1-deficient mice. *Am. J. Pathol.* **175**, 2540–2556
31. Kirkegaard, T., Roth, A. G., Petersen, N. H., Mahalka, A. K., Olsen, O. D., Moilanen, I., Zylicz, A., Knudsen, J., Sandhoff, K., Arenz, C., Kinnunen, P. K., Nylandsted, J., and Jäättelä, M. (2010) Hsp70 stabilizes lysosomes and reverts Niemann-Pick disease-associated lysosomal pathology. *Nature* **463**, 549–553
32. Appelqvist, H., Nilsson, C., Garner, B., Brown, A. J., Kågedal, K., and Ollinger, K. (2011) Attenuation of the lysosomal death pathway by lysosomal cholesterol accumulation. *Am. J. Pathol.* **178**, 629–639
33. Prinetti, A., Prioni, S., Chiricozzi, E., Schuchman, E. H., Chigorno, V., and Sonnino, S. (2011) Secondary alterations of sphingolipid metabolism in lysosomal storage diseases. *Neurochem. Res.* **36**, 1654–1668
34. Devlin, C., Pipalia, N. H., Liao, X., Schuchman, E. H., Maxfield, F. R., and Tabas, I. (2010) Improvement in lipid and protein trafficking in Niemann-Pick C1 cells by correction of a secondary enzyme defect. *Traffic* **11**, 601–615
35. Jones, I., He, X., Katouzian, F., Darroch, P. I., and Schuchman, E. H. (2008) Characterization of common SMPD1 mutations causing types A and B Niemann-Pick disease and generation of mutation-specific mouse models. *Mol. Genet. Metab.* **95**, 152–162
36. Graber, D., Salvayre, R., and Levade, T. (1994) Accurate differentiation of neuronopathic and nonneuronopathic forms of Niemann-Pick disease by evaluation of the effective residual lysosomal sphingomyelinase activity in intact cells. *J. Neurochem.* **63**, 1060–1068
37. Ledesma, M. D., Prinetti, A., Sonnino, S., and Schuchman, E. H. (2011) Brain pathology in Niemann-Pick disease type A: insights from the acid sphingomyelinase knockout mice. *J. Neurochem.* **116**, 779–788
38. García-Ruiz, C., Colell, A., Mari, M., Morales, A., Calvo, M., Enrich, C., and Fernández-Checa, J. C. (2003) Defective TNF- α -mediated hepatocellular apoptosis and liver damage in acidic sphingomyelinase knockout mice. *J. Clin. Invest.* **111**, 197–208